Proceedings of ALGORITMY 2016
pp. 1–10

FRACTIONAL DERIVATIVES FOR VORTEX SIMULATIONS

BÉLA J. SZEKERES * AND FERENC IZSÁK †

Abstract. Two modifications of the incompressible Navier–Stokes equations are investigated. The first modification is based on assuming hyperviscosity such that the Laplacian operator is replaced with a fractional Laplacian. In the second modification consists of using fractional time derivatives. Both models are tested on the classical Backward Facing Step benchmark problem with different expansion ratios. The simulation results are in a good accordance with real measurements.

Key words. turbulence, fractional derivatives, fractional Laplacian

AMS subject classifications. 15A15, 15A09, 15A23

1. Introduction. The Navier–Stokes equations for the velocity field $\mathbf{u} : \Omega \to \mathbb{R}^2$ of an incompressible fluid are given as

$$\begin{aligned} \frac{\partial \mathbf{u}}{\partial t} &= (-\mathbf{u} \cdot \nabla)\mathbf{u} - \nabla p + \nu \Delta \mathbf{u} \\ \nabla \cdot \mathbf{u} &= 0. \end{aligned} \tag{1.1}$$

For most fluids the kinematic viscosity ν is very small compared to the other terms. A corresponding numerical model has to resolve at least down to the viscosity lengthscale: for example, the air's viscosity lengthscale is in the millimeter range while the energy-carrying lengthscales are up to thousands of kilometres [1]. To save computational cost, we have to bring the dissipation lengthscales closer to the grid scale in a spatial discretization. To achieve this two ways are offered nowadays. The first one is the eddy viscosity conception. Shortly, this model increases the kinematic viscosity, which results in larger viscous forces. Another option which we use here is to replace the viscosity term with a hyperviscosity term $-\nu_h(-\Delta)^\alpha$, where $\alpha \geq 1$. If the flow approaches a steady state we can also try to stabilize the corresponding numerical simulations using fractional time derivatives. The aim of this contribution is to introduce the above modifications of the incompressible Navier–Stokes equations for an efficient and accurate numerical simulation of vortices.

Model 1: Fractional hyperviscosity. In our hyperviscosity model we do not change the viscosity coefficient but we let the power of the Laplacian operator to be non-integer:

$$\begin{aligned} \frac{\partial \mathbf{u}}{\partial t} &= (-\mathbf{u} \cdot \nabla)\mathbf{u} - \nabla p - \nu(-\Delta)^\alpha \mathbf{u} \\ \nabla \cdot \mathbf{u} &= 0. \end{aligned} \tag{1.2}$$

We show on the well-known Backward Facing Step (BFS) benchmark problem that α can be chosen according to real measurements.

*Department of Applied Analysis and Computational Mathematics & MTA-ELTE NumNet Research Group, Eötvös Loránd University, Pázmány P. stny. 1/C, 1117 Budapest (szbpagt@cs.elte.hu).

†(izsakf@cs.elte.hu)

Model 2: Time-fractional Navier–Stokes equations. In many real situations, after some time the flow becomes almost steady-state such that the time derivative is negligible. Accordingly, for some applications only a stationary solution of (1.1) is investigated. For a coarse spatial discretization the numerical solution of this problem can be highly inaccurate. To avoid this we propose to replace the time derivative in with (1.2) with $\frac{\partial^\beta \mathbf{u}}{\partial t^\beta}$ for some $\beta \in (0,1)$ rather than take the stationary equation. Since the fractional order time derivative is a non-local operator, and can be given as a limit of linear combination of past values, we expect that this stabilizes the time integration in the numerical solutions.

In concrete terms we investigate the following problem on Ω:

$$\begin{aligned} \frac{\partial^\beta \mathbf{u}}{\partial t^\beta} &= (-\mathbf{u}\cdot\nabla)\mathbf{u} - \nabla p + \nu\Delta\mathbf{u} \\ \nabla\cdot\mathbf{u} &= 0, \end{aligned} \tag{1.3}$$

where the boundary conditions will be specified later. We test this model also on the Backward Facing Step benchmark problem and point out that numerical simulations are in good accordance with some real measurements [9], [10], [14], [15].

2. Main results. In this section we summarize the results for the new models. In both cases we start with some mathematical preliminaries.

2.1. The model with fractional hyperviscosity. For a given right hand side $f \in L_2(\Omega)$ the solution operator of the boundary value problem

$$\begin{aligned} -\Delta u &= f \quad \text{in } \Omega \\ u &= 0 \quad \text{on } \partial\Omega \end{aligned} \tag{2.1}$$

can be recognized as $(-\Delta_{\mathcal{D}})^{-1} : L_2(\Omega) \to L_2(\Omega)$, which is a compact, self-adjoint operator.

The Hilbert–Schmidt theory of compact operators (see, *e.g.*, [3], Section 6.2) implies the existence of the complete system $\{\phi_j\}_{j\in Z^+}$ of its eigenfunctions with the eigenvalues $0 < \mu_1 \le \mu_2 \le \dots$. With these $f = \sum_{j=1}^\infty f_j\phi_j$ denotes the Fourier expansion of f. We also use the notation $\lambda_j := \frac{1}{\mu_j}$ for $j \in \mathbb{N}^+$.

Definition 2.1. *Let us introduce the linear space*

$$D_s := \left\{ f \in L_2(\Omega) : \sum_{j=1}^\infty f_j^2 \lambda_j^s < \infty \right\}$$

and $(-\Delta)^\alpha : D_{2\alpha} \to L_2(\Omega)$ *for* $\alpha > 0$ *with*

$$(-\Delta)^\alpha f := \sum_{j=1}^\infty f_j \lambda_j^\alpha \phi_j \quad \textit{and} \quad |f|^2_{D_{2\alpha}} := \sum_{j=1}^\infty f_j^2 \lambda_j^{2\alpha}.$$

Using this definition the viscous term in (1.1) is replaced with a hyperviscous term to get the following equations:

$$\begin{aligned} \frac{\partial \mathbf{u}}{\partial t} &= (-\mathbf{u}\cdot\nabla)\mathbf{u} - \nabla p - \nu(-\Delta)^\alpha \mathbf{u}, \quad \alpha \ge 1 \\ \nabla\cdot\mathbf{u} &= 0. \end{aligned} \tag{2.2}$$

To discretize (2.2) we use the method of the work [2], which is a finite difference approximation on a staggered grid. The semidiscretization results in the following ODE:

$$\begin{aligned} \vec{u}_t + L_h(\vec{u})\vec{u} + \mathrm{grad}_h p &= \mathbf{0}, \\ \mathrm{div}_h \vec{u} &= 0, \end{aligned} \tag{2.3}$$

where $L_h(\vec{u}) = D_h(\vec{u}) + \nu(-\Delta_h)^\alpha$, $D_h(\vec{u})\vec{u}$ is the approximation of the nonlinear terms, div_h is the discrete divergence and grad_h is the discrete gradient operator. To approximate the operator $(-\Delta)^\alpha$, the so-called matrix transform (or matrix transfer) method (MTM) has been proposed in [6], [16] and [17] and generalized in [18] for time and space-fractional diffusion problems. This approach makes possible to compute with the sparse matrix $-\Delta_h$ corresponding to the standard Laplacian operator $-\Delta$. A corresponding error analysis was carried out for the finite element methods with respect to the L_2-norm [7] and for the finite difference methods with respect to the $L_{2,h}$-norm [8].

The fractional power α of a matrix can be defined and approximated in several ways, see [19]. Since we only focus to the power of symmetric positive definite matrices the following simple algorithm is applied:

1. Compute the decomposition $VDV^{-1} = -\Delta_h$, where the columns of V are the eigenvectors of $-\Delta_h$ and D is a diagonal.

2. Take the power of the diagonal elementwise so that $(-\Delta_h)^\alpha = VD^\alpha V^{-1}$.

Indeed, we have to compute vectors of form $(-\Delta_h)^{-\alpha}\vec{u}$ by solving linear problems with the matrix $(-\Delta_h)^\alpha$. For this an efficient algorithm is proposed in [18].

We solve then (2.3) using a simple predictor-corrector algorithm introduced by Patankar [5]. We start from an initial velocity field $\vec{u}^0$ and an initial value for the pressure p^0 and apply the time step τ. The main steps of the algorithm are the following.

1. Solve the following equation for $\vec{w}$:

$$\frac{\vec{w} - \vec{u}^n}{\tau} + L_h(\vec{u}^n)\vec{w} + \mathrm{grad}_h p^n = 0. \tag{2.4}$$

2. Solve the following equation for q:

$$\mathrm{div}_h \mathrm{grad}_h q = \frac{1}{\tau}\mathrm{div}_h \vec{w}.$$

3. Compute the pressure values $p^{n+1} = q + p^n$.
4. Compute the velocity vector $\vec{u}^{n+1} = \vec{w} - \tau \mathrm{grad}_h q$.

2.2. Time-fractional Navier–Stokes equations. For this model we use the time-fractional derivative, see also [4].

Definition 2.2. *For functions $f : \mathbb{R} \to \mathbb{R}$ the time-fractional derivative of order $0 < \beta \leq 1$ is defined as*

$$\frac{\partial^\beta f(t)}{\partial t^\beta} := \lim_{N\to\infty} \Big\{ \sum_{k=0}^{N} \binom{\beta}{k} (-1)^k \frac{f(t-kh)}{h^\beta} \Big\}$$

provided that the limit exists.

With this, we investigate the following problem:

$$\begin{aligned} \frac{\partial^\beta \mathbf{u}}{\partial t^\beta} &= (-\mathbf{u}\cdot\nabla)\mathbf{u} - \nabla p + \nu\Delta\mathbf{u} \\ \nabla\cdot\mathbf{u} &= 0, \end{aligned} \tag{2.5}$$

which will be equipped with appropriate boundary conditions.

Our numerical method follows the approach in [2] and based on the semidiscretization of (2.5):

$$\begin{aligned} D_{\tau,\beta}\vec{u} + L_h(\vec{u})\vec{u} + \mathrm{grad}_h p &= \mathbf{0}, \\ \mathrm{div}_h\vec{u} &= 0, \end{aligned} \tag{2.6}$$

where for the time step $\tau = \frac{t}{N}$ we use

$$D_{\tau,\beta}f(t) = \sum_{k=0}^{N}\binom{\beta}{k}(-1)^k\frac{f(t-k\tau)}{\tau^\beta}.$$

Starting again from the initial values $\vec{u}^0$ and p^0 the n-th time step to solve (2.6) numerically consists of the following:

1. Solve equation (2.7) for $\vec{w}$:

$$\frac{\vec{w} - \sum_{k=1}^{n}\binom{\beta}{k}(-1)^{k+1}\vec{u}^{n-k}}{\tau^\beta} + L_h(\vec{u}^n)\vec{w} + \mathrm{grad}_h p^n = 0. \tag{2.7}$$

2. Solve the following equation for q:

$$\mathrm{div}_h\mathrm{grad}_h q = \frac{1}{\tau^\beta}\mathrm{div}\vec{w}.$$

3. Compute the pressure values $p^{n+1} = q + p^n$.
4. Compute the velocity vector $\vec{u}^{n+1} = \vec{w} - \tau^\beta\mathrm{grad}_h q$.

Computing with this algorithm for several values of β we are looking for the minimal right-hand side. This corresponds to the quasi steady-state solution.

3. Numerical experiments.

3.1. Discretization operators. We use here the notation $\mathbf{u} = (u, v)^T$ for the velocity field both at the continuous and the discrete level. Following the method in [2], we use an equidistant staggered grid, where we compute on different grid points which are associated to u, v and p, respectively, see Fig. 3.1. For simplicity we give the details of the discretization only for the horizontal velocity components in the grid points associated to u; for further details we refer to [2].

Spatial discretization operators. We approximate the *pressure term* $\frac{\partial p}{\partial x}$ using the operator grad_h as follows:

$$\left.\frac{\partial p}{\partial x}\right|_{i,j+1/2} \approx \big(\mathrm{grad}_h p\big)_{i,j+1/2} := \frac{1}{h}\big(p_{i+1/2,j+1/2} - p_{i-1/2,j+1/2}\big).$$

The *viscous term* Δu is discretized with the operator Δ_h in the following way.

$$\begin{aligned} \Delta u\Big|_{i,j+1/2} \approx \big(\Delta_h u\big)_{i,j+1/2} := \frac{1}{h^2}\big(u_{i+1,j+1/2} - 2u_{i,j+1/2} + u_{i-1,j+1/2}\big) \\ + \frac{1}{h^2}\big(u_{i,j+3/2} - 2u_{i,j+1/2} + u_{i,j-1/2}\big). \end{aligned}$$

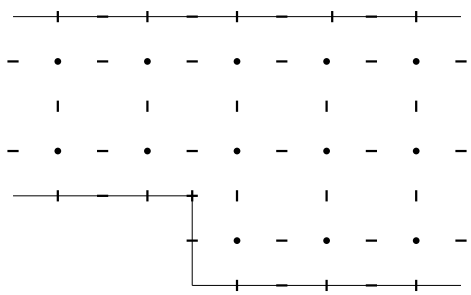

FIG. 3.1. *Staggered grid in the computations. Grid points with "–" are indexed by* $(i, j+1/2)$ *and associated to* u*; those with "|" are indexed by* $(i+1/2, j)$ *and associated to* v *and those with "•" are indexed by* $(i+1/2, j+1/2)$ *and associated to* p*.*

In the discretization of the *convective term* $(\mathbf{u}\cdot\nabla)\mathbf{u}$ we discuss its horizontal component $u\frac{\partial u}{\partial x}+v\frac{\partial u}{\partial y}$. This is approximated with operator $D_h(\mathbf{u})$ defined as follows:

$$u\frac{\partial u}{\partial x}+v\frac{\partial u}{\partial y}\Big|_{i,j+1/2}\approx \big(D_h(\mathbf{u})u\big)_{i,j+1/2}:=\frac{1}{h}\Big[\Big(\frac{u_{i+1,j+1/2}+u_{i,j+1/2}}{2}\Big)^2 -\Big(\frac{u_{i-1,j+1/2}+u_{i,j+1/2}}{2}\Big)^2\Big]+\frac{1}{h}\Big[\Big(\frac{v_{i-1/2,j+1}+v_{i+1/2,j+1}}{2}\Big)\Big(\frac{u_{i,j+1/2}+u_{i,j+3/2}}{2}\Big) -\Big(\frac{v_{i-1/2,j}+v_{i+1/2,j}}{2}\Big)\Big(\frac{u_{i,j+1/2}+u_{i,j-3/2}}{2}\Big)\Big].$$

We finally we approximate the *divergence operator* in the points associated to p as follows:

$$\mathrm{div}\mathbf{u}\Big|_{i+1/2,j+1/2}\approx\Big(\mathrm{div}_h\mathbf{u}\Big)_{i+1/2,j+1/2}:=\frac{1}{h}\big(u_{i+1,j+1/2}-u_{i,j+1/2}\big) +\frac{1}{h}\big(v_{i+1/2,j+1}-v_{i+1/2,j}\big).$$

3.2. Parameters in the simulation. We test our models on a classical Backward Facing Step benchmark problem. For this we use the real measurements of the works [9], [10], [14], [15] and we also compare our simulation results with other numerical predictions in [10],[11], [12],[13]. The geometric setup of this problem is shown in Fig. 3.2.

In the model problem, the fluid flows into the channel at the upper left side and it flows out at the right-hand side. The Reynolds number based on the hydraulic diameter of the inlet channel is $\mathrm{Re}_D=\frac{4hv_{\max}}{3\nu}$, where D means the hydraulic diameter of the inlet channel $D=2h$. With these the exact boundary conditions are the following:

1. $x=-l, y\in[H-h,h]$ (inflow section): $v_y=0$ and $v_x=-\frac{4(H-y)(H-h-y)}{h^2}v_{\max}$
2. $x=L-l$ (outflow section): $\frac{\partial v_x}{\partial x}=\frac{\partial v_y}{\partial x}=0$ and $p=0$,
3. on the remaining part of the boundary: $v_x=v_y=0$.

We also used a short inlet channel. Whenever the problem seems to be easy, many recent calculations result in an inaccurate prediction of certain well-measurable quantities, such as the location of the so-called reattachment lengths r, s and rs. For a

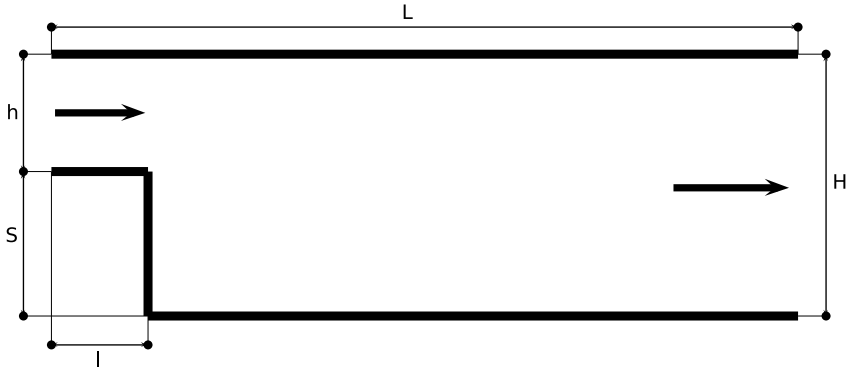

FIG. 3.2. *The Backward Facing Step problem: a flow is investigated in the composition of two rectangular channels. The diameter h of the inlet channel is smaller that the diameter H of the outlet channel. Non-slip boundary conditions are applied at the solid walls.*

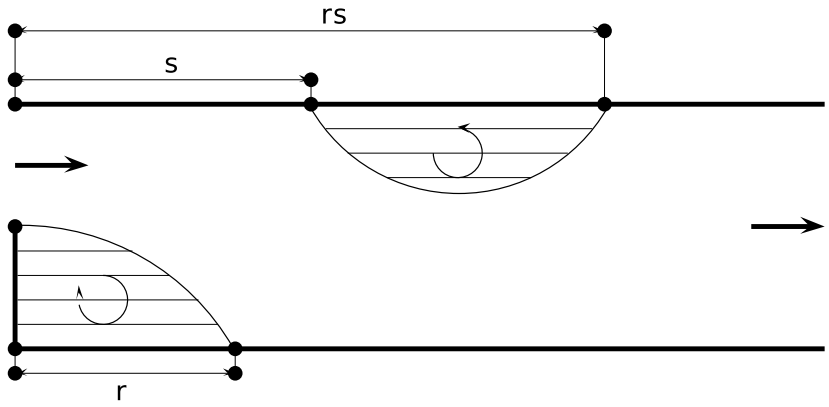

FIG. 3.3. *Reattachment lengths r, s and rs. The subdomains of the computational domain with $v_x < 0$ are shaded.*

TABLE 3.1
Numerical results for time–fractional Navier–Stokes equations, SST=Shear Stress Modell, DNS=Direct Numerical Simulation, SA=Spalart–Allmaras model, k–ϵ=k–ϵ-model, ER=Expansion ratio H/h

Re	ER	Measured r/S	Numerical simulations	Our result	β
2425	1.66	9.2 [10]	SST 9.4, SA 8.54, RNG k–ϵ 6.93, k–ϵ 6.3 [10]	8.2	0.75
2976	1.66	7.6 [10]	SST 7.89, SA 6.93, RNG k–ϵ 5.98, k–ϵ 5.1 [10]	7.6	0.7
3615	1.66	6.45 [10]	SST 6.57, SA 5.89, RNG k–ϵ 5.32, k–ϵ 4.2 [10]	6.5	0.65
5000	1.2	6.0 [14]	DNS 6.0 [11]	5.9	0.55
8000	1.942	8.0 [9]	k–ϵ 6.8 [12]	7.52	0.75
132000	1.5	7.0 [15]	k–ϵ 5.8 [15]	6.6	0.75

visualization of these we refer to Fig. 3.3 and a typical simulation result with the computed velocity field is shown in Fig. 3.4.

We have chosen in every test case the time step $\tau = 1.25 \cdot 10^{-3}$, the kinematic viscosity $\nu = \frac{2}{30}$, the step height and the inlet channel length $S = 0.5$ and the grid

TABLE 3.2
Numerical results for hyperviscous Navier–Stokes equations, SST=Shear Stress Modell, DNS=Direct Numerical Simulation, SA=Spalart–Allmaras model, k–ϵ=k–ϵ-model, ER=Expansion ratio H/h

Re	ER	Measured r/S	Numerical simulations	Our result	α
2425	1.66	9.2 [10]	SST 9.4, SA 8.54, RNG k–ϵ 6.93, k–ϵ 6.3 [10]	9.0	2.2
2976	1.66	7.6 [10]	SST 7.89, SA 6.93, RNG k–ϵ 5.98, k–ϵ 5.1 [10]	6.7	2.45
3615	1.66	6.45 [10]	SST 6.57, SA 5.89, RNG k–ϵ 5.32, k–ϵ 4.2 [10]	6.0	2.6
5000	1.2	6.0 [14]	DNS 6.0 [11]	6.06	2.45
8000	1.942	8.0 [9]	k–ϵ 6.8 [12]	8.4	1.8
132000	1.5	7.0 [15]	k–ϵ 5.8 [13]	6.6	1.7

parameter $h = 0.05$. The main channel length was $L - l = 10$, except of the case $\mathrm{Re} = 5000$, where we used a shorter channel length $L - l = 5$. The optimal parameters α and β were selected using the result of consecutive simulations.

Note that in the hyperviscosity model the increasing of the values α always make the scheme more stable. At the same time, too large values of this value result in the decreasing of the reattachment length and make the simulation results unrelaible. We found that optimal values of α fall in the range $(1.7, 2.6)$ for large Reynolds numbers. At the same time, the results were not much sensitive to this parameter in the above range.

We have similar experience by choosing the optimal parameters β. Small values of β can result in unstable simulations for large Reynolds numbers. At the same time, the result for the reattachment lengths is only realistic if β is below the threshold 0.8. In contrast to the above parameter, the results are rather sensitive to the variation of β, we found that these parameters should lie in the range $(0.55, 0.75)$.

We found also that an optimal choice of α and β does not significantly depend on the Reynolds number, which is a favorable property.

Our results using the time-fractional Navier–Stokes equations are summarized in Table (3.1) and the results using the hyperviscous model can be found in Table (3.2). Note that Reynolds numbers can be calculated differently: the Reynolds numbers in the tables are the original values in the corresponding articles. Table (3.3) shows how to switch these values to Re_D in our calculations. Our simulation results are in a good agreement with measured data in the sense that the relative error rate in the main reattachment length r is within 10%.

TABLE 3.3
Converting the different Reynolds numbers to Re_D, which is used in our simulations and based on the hydraulic diameter of the inlet channel

Re in the articles	Re_D
2425	4850
2967	5952
3615	7230
5000	26666
8000	8000
132000	533333

Conclusion. We investigated two modifications of the two-dimensional incompressible Navier–Stokes equations. Firstly, the Laplacian operator was replaced with

a fractional Laplacian, while in the second model a fractional time derivative was used. Both models were tested on the classical Backward Facing Step benchmark problem with different expansion ratios. We found that the fractional parameters can be tuned so that the simulation results are in a good accordance with real measurements regarding the main reattachment length r. In each case, the relative error rate for this quantity is below 10%. Since these approaches lead to an accurate simulation of single vortices, we can hope that are useful for the simulation of turbulent flows.

Acknowledgments. The authors acknowledge the financial support of the Hungarian National Research Fund OTKA (grant K112157).

REFERENCES

[1] K. Spyksma, M. Magcalas, N. Campbell, *Quantifying effects of hyperviscosity on isotropic turbulence*, Physics of Fluids, 24, 12 (2012)
[2] Harlow, F. H., Welch, E. J.: Numerical Calculation of Time-Dependent Viscous Incompressible Flow with Free Surface, The Physics of Fluids 8,12, 2182–2189 (1965)
[3] F. Hirsch, G. Lacombe, *Elements of Functional Analysis*, Graduate Texts in Mathematics, Springer-Verlag, New York, 192 (1993)
[4] I. Podlubny, *Fractional Differential Equations*, Academic Press Inc., San Diego, CA (1999)
[5] S. V. Patankar, D. B. Spalding, *A calculation procedure for heat, mass and momentum transfer in three–dimensional parabolic flows*, Int. J. Heat and Mass Transfer 15, 1787–1806 (1972)
[6] M. Ilic, F. Liu, I. Turner, V. Anh, *Numerical approximation of a fractional-in-space diffusion equation. I*, Fract. Calc. Appl. Anal., 8, 323–341 (2005)
[7] B. J. Szekeres, F. Izsák, *Finite element approximation of fractional order elliptic boundary value problems*, J. Comput. Appl. Math., 292, 553–561 (2016)
[8] B. J. Szekeres, F. Izsák, *Numerical solution of the twodimensional fractional diffusion equation on a general domain*, manuscript
[9] B. F. Armaly, F. Durst, J. C. F. Pereira, B. Schnung, *Experimental and theoretical investigation of backward-facing step flow*, 127, 473–496 (1983)
[10] Anwar-ul-Haque, F. Ahmad, S. Yamada, S. R. Chaudhry, *Assessment of Turbulence Models for Turbulent Flow over Backward Facing Step*, Proceedings of the World Congress on Engineering 2007 Vol II, (2007)
[11] H. Le, P. Moin, J. Kim, *Direct numerical simulation of turbulent flow over a backward-facing step*, J. Fluid Mech., 330, 349–374 (1997)
[12] L. Jongebloed, *Numerical Study using FLUENT of the Separation and Reattachment Points for Backwards-Facing Step Flow*, Masters Project, (2008)
[13] S. Thangam, N. Hur, *A highly-resolved numerical study of turbulent separated flow past a backward-facing step*, International Journal of Engineering Science, 29, 5, 607–615 (1991)
[14] S. Jovic, D. M. Driver, *Backward-facing step measurements at low Reynolds number, $Re_h =$ 5000*, NASA STI/Recon Technical Report N, 94, 33290 (1994)
[15] J. Kim, S. J. Kline, J. P. Johnston, *Investigation of a Reattaching Turbulent Shear Layer: Flow Over a Backward-Facing Step*, J. Fluids Eng. 102, 3, 302–308 (1980)
[16] M.Ilić, F. Liu, I. Turner, V. Anh, *Numerical approximation of a fractional-in-space diffusion equation. II. With nonhomogeneous boundary conditions*, Fract. Calc. Appl. Anal., 9, 4, 333-349 (2006)
[17] F. Liu, P. Zhuang, V. Anh, I. Turner, *A fractional-order implicit difference approximation for the space-time fractional diffusion equation*, ANZIAM J., 47, C48–C68 (2005)
[18] M. Ilić, I. W. Turner, D. P. Simpson, *A restarted Lanczos approximation to functions of a symmetric matrix*, IMA J. Numer. Anal., 30, 4, 1044–1061 (2010)
[19] N. J. Higham, L. Lin, *An improved Schur–Padé algorithm for fractional powers of a matrix and their Fréchet derivatives*, SIAM J. Matrix Anal. Appl., 34, 3, 1341–1360 (2013)

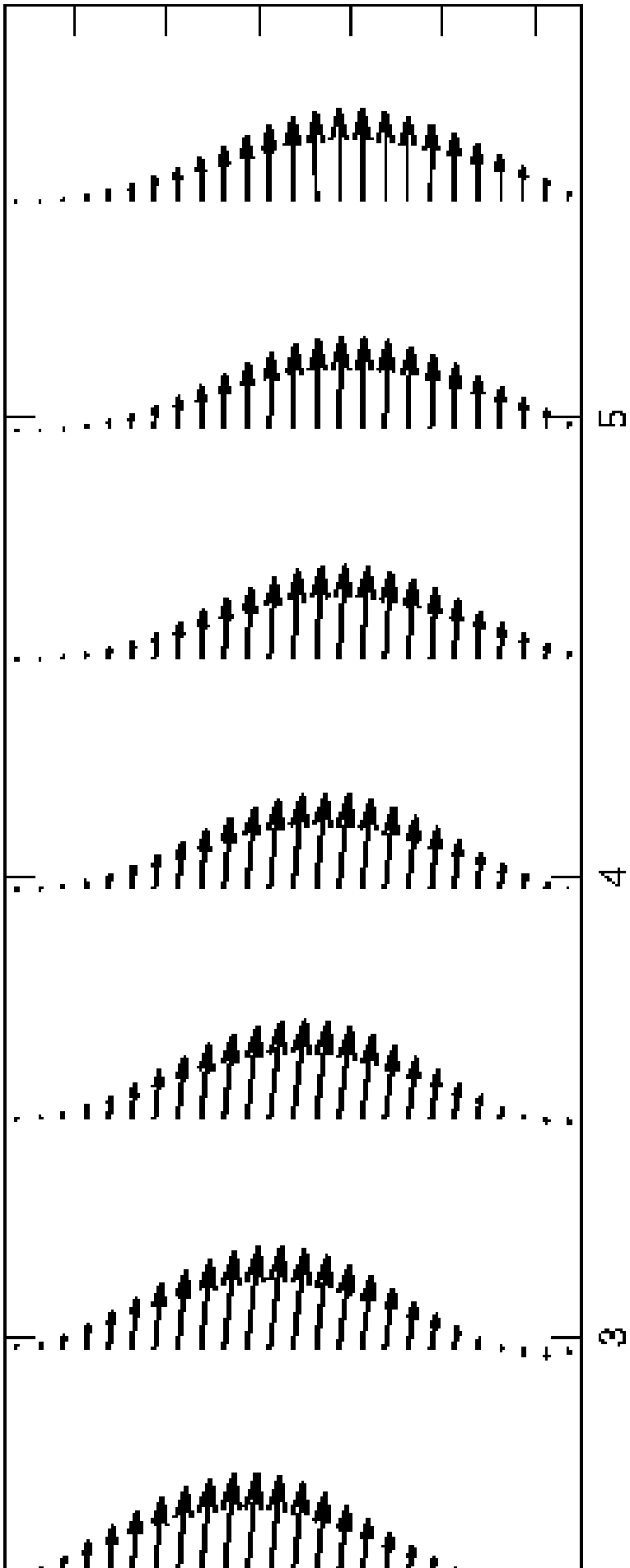
5
4
3